NANO LETTERS

Letter

pubs.acs.org/NanoLett

Fabrication of Nonperiodic Metasurfaces by Microlens Projection Lithography

Mathieu Gonidec,[†] Mahiar M. Hamedi,[†] Alex Nemiroski,[†] Luis M. Rubio,[†] Cesar Torres,[†] and George M. Whitesides*[,†,‡,§]

[†]Department of Chemistry and Chemical Biology, Harvard University, 12 Oxford Street, Cambridge, Massachusetts 02138, United States

[‡]Wyss Institute for Biologically Inspired Engineering, Harvard University, 60 Oxford Street, Cambridge, Massachusetts 02138, United States

[§]Kavli Institute for Bionano Science and Technology, Harvard University, 29 Oxford Street, Cambridge, Massachusetts 02138, United States

Supporting Information

ABSTRACT: This paper describes a strategy that uses template-directed self-assembly of micrometer-scale microspheres to fabricate arrays of microlenses for projection photolithography of periodic, quasiperiodic, and aperiodic infrared metasurfaces. This method of "template-encoded microlens projection lithography" (TEMPL) enables rapid prototyping of planar, multiscale patterns of similarly shaped structures with critical dimensions down to ~400 nm. Each of these structures is defined by local projection lithography with a single microsphere acting as a lens. This paper explores the use of TEMPL for the fabrication of a broad range of two-dimensional lattices with varying types of nonperiodic spatial distribution. The matching optical spectra of the fabricated and simulated metasurfaces confirm that TEMPL can produce structures that conform to expected optical behavior.

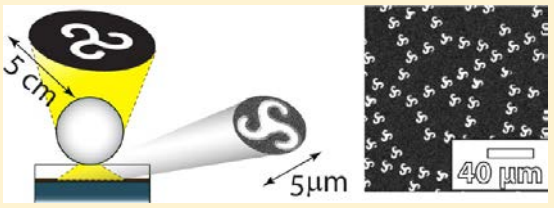

KEYWORDS: *Microfabrication, self-assembly, microlens lithography, metamaterials*

Optical metasurfaces, periodic,[1−3] quasiperiodic, or aperiodic[4] patterns of nanoscale metal or dielectric features with subwavelength spacing, enable a degree of engineered control over local and scattered electromagnetic fields not possible with naturally occurring materials.[5] These optically thin materials have the potential to become fundamental components in sensitive chemical and biological sensors[6−11] and flat optics.[12−14] Despite many recent advances, available methods cannot fabricate new designs with the required feature sizes both rapidly and over moderate areas (~mm^2−cm^2). There are many strategies (see Table S1) for fabricating nanomaterials, each with their own advantages and disadvantages. Serial methods, such as direct-write photo-, electron-, and ion-beam lithography, and dip-pen lithography may offer high resolution but are typically slow and expensive or require specialized instruments. Parallel methods of fabrication, such as mask-based photolithography (e.g., contact or projection lithography), nanoimprint lithography, and microcontact printing, are suited to high-throughput manufacturing but they still require high-resolution serial fabrication of the required masks or masters. None of these techniques is ideally suited for academic research on metasurfaces because efficient iteration between theory and experiment requires generation of new designs rapidly over large areas and at low cost.

This limitation has slowed the comparison of theory and experiment. This paper describes a method for fabricating infrared metasurfaces that combines the simplicity of self-assembly with the precision of projection lithography to offer new capabilities in the rapid-prototyping of periodic and quasiperiodic metasurfaces, particularly those with feature sizes in the range of 0.4−10 μm. While it requires a high-resolution master for templating an array of microspheres corresponding to the desired distribution of features, it enables rapid iteration between different designs of the unit cell without changing the master template.

This method combines two strategies. The first, microlens projection lithography, uses self-assembled arrays of colloidal microlenses that each project an image of a distant, macroscopic mask onto the substrate.[15−17] It enables efficient fabrication of arrays of microstructures (colloidal self-assembly can be rapid) and more importantly rapid iteration between different masks. The second strategy is to use self-assembled arrays of silica spheres as microlenses and to template the placement of these spheres. The silica spheres act as lenses with high NA (~0.8) and enable spatial resolution down to ~0.3 μm. Because the microlenses are small (typically around 5 μm in diameter) and the pattern being projected is large (typically around 5 cm in size) the projected image is greatly reduced in

Received: March 4, 2016
Revised: May 24, 2016
Published: May 31, 2016

DOI: 10.1021/acs.nanolett.6b00952
Nano Lett. 2016, 16, 4125−4132

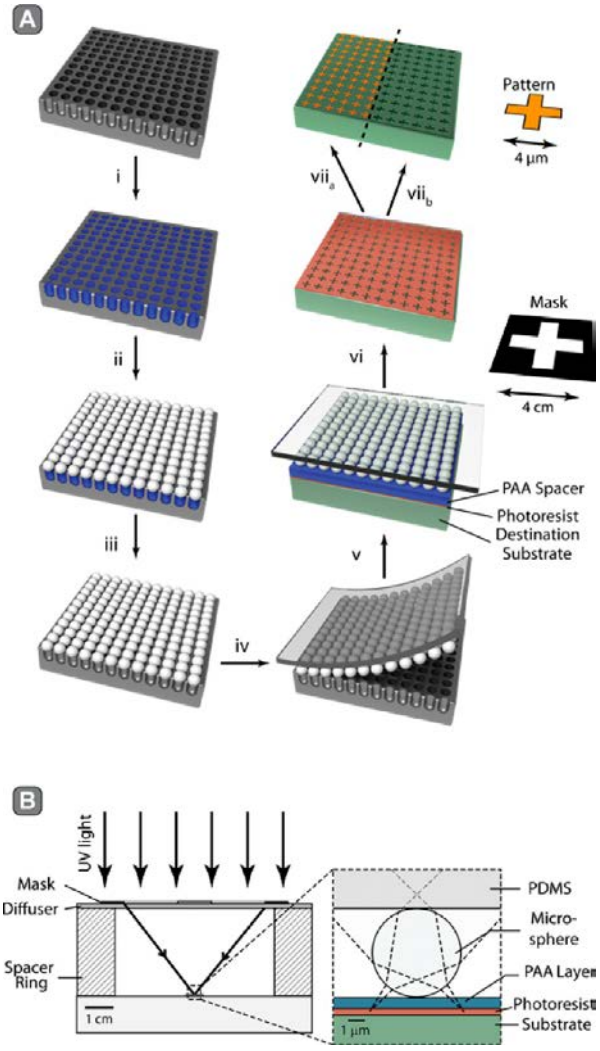

Figure 1. Schematic diagram of the templated microlens process flow (A) from the template in silicon to the final substrate. (i) The wells in the silicon wafer are filled with PEI, (ii) the beads are selectively adhered inside the wells due to their adhesion to PEI, (iii) the PEI is removed by thermal decomposition with a butane torch, (iv) the beads are picked up with a PDMS slab, (v) the array of beads is placed in contact with the substrate, (vi) the exposure is performed through the PDMS and the spheres, and the sample is developed, (vii) the pattern is transferred by metallization and lift off (a) or by etching (b). (B) Schematic diagram of the projection lithography setup. An intense source of noncollimated UV-light impinges on the cm-scale photomask, and the transmitted light is focused by the lensing of each microsphere onto the underlying photoresist to create a replica of the features of the mask.

size (~10,000×, relative to the photomask) in a single step. This characteristic relaxes the requirements for the resolution of the photomask to values >1 mm, features easily fabricated by conventional printing or laser-cutting; e-beam or laser writing methods are not required.

The combination of these two strategies, which we call "template-encoded microlens projection lithography" (TEMPL), overcomes one of the major challenges in fabrication of metasurfaces: rapid evolution in the content of the unit cell. TEMPL uses a master template, fabricated by direct-write photolithography, to template the position of the silica microspheres in the desired planar arrangement of microlenses. Here, we demonstrate that TEMPL can be used to fabricate periodic and quasiperiodic patterns of unit cells that are either indistinguishable or very similar with characteristics necessary for the development of infrared metasurfaces. Although, TEMPL is not suitable for the fabrication of metasurfaces that require changes in the shape of the unit cell, the method is particularly well suited to investigate the influence of the global spatial distribution of "unit cells" on the optical properties of a material. Furthermore, this work demonstrates for the first time (to our knowledge) template-directed assembly of micron-scale, complex arrays of spheres coupled with the transfer of these patterns to flat, optically transparent substrates.

In the TEMPL process, a template consisting of cylindrical wells etched in a planar silicon wafer directs the self-assembly of dry, SiO_2 microspheres, which are then transferred to an optically transparent substrate on which they serve as microlenses for projection lithography. We first prepared a master template by standard direct-write photolithography, followed by reactive ion etching. This step was the most demanding one from the point of view of instrumentation but can easily be outsourced to commercial vendors. We fabricated cylindrical wells with a width of approximately 95% and a depth of 50% of the diameter of the microspheres. Our method of templating with this master was inspired in part by a protocol described by Yoon et al.,[18] which we modified and expanded into a four-step process that yielded consistently reproducible, high-quality patterns. Figure 1a shows a schematic of this procedure. (i) After placing the template on a hard surface, we first selectively filled the wells in the master with polyethylenimine (PEI), which served as an adhesive for the spheres, by applying a viscous solution of PEI to the patterned areas of the master with a disposable wooden stick and then wiping away the excess present on the surface of the wafer between the wells with smooth, linear strokes, using either a damp, dust-free cloth or a dust-free swab (clean room grade) that was dipped in deionized water. This step removed the PEI from the areas of the master template between the wells, while leaving the wells filled. (ii) We then deposited dry, monodisperse, silica microspheres onto the master (a few milligrams per cm^2) and used a clean piece of PDMS (of approximately 2 × 2 × 0.3 cm) to apply a gentle pressure with 1−2 fingers and to rub the microspheres against the templates in circular motion until all silica spheres appeared to be removed from the unpatterned areas. The spheres adhered selectively to the PEI inside the wells; continual rubbing removed excess spheres. Removal of the small amount of remaining untemplated spheres was aided by carefully introducing a gentle stream of nitrogen. This step was the most empirical part of the process and required significant practice to produce high quality filling with few errors. (iii) We next heated the back of the silicon master with a butane torch to burn off the PEI adhesive. Alternatively, the removal of the PEI can also be achieved by placing the silicon master in a laboratory oven at 500 °C for 1 h. At the conclusion of this procedure, the microspheres remained positioned on top of, and centered on the wells, but they no longer adhered to the substrate and were free to be transferred to another surface. Importantly, we chose a well size slightly smaller than the microspheres to ensure that they did not fall entirely into the wells. (iv) We finally transferred the microspheres to an intermediate surface by placing a thin, flat slab of clean PDMS on top of the microspheres, applying gentle pressure, and

DOI: 10.1021/acs.nanolett.6b00952
Nano Lett. 2016, 16, 4125−4132

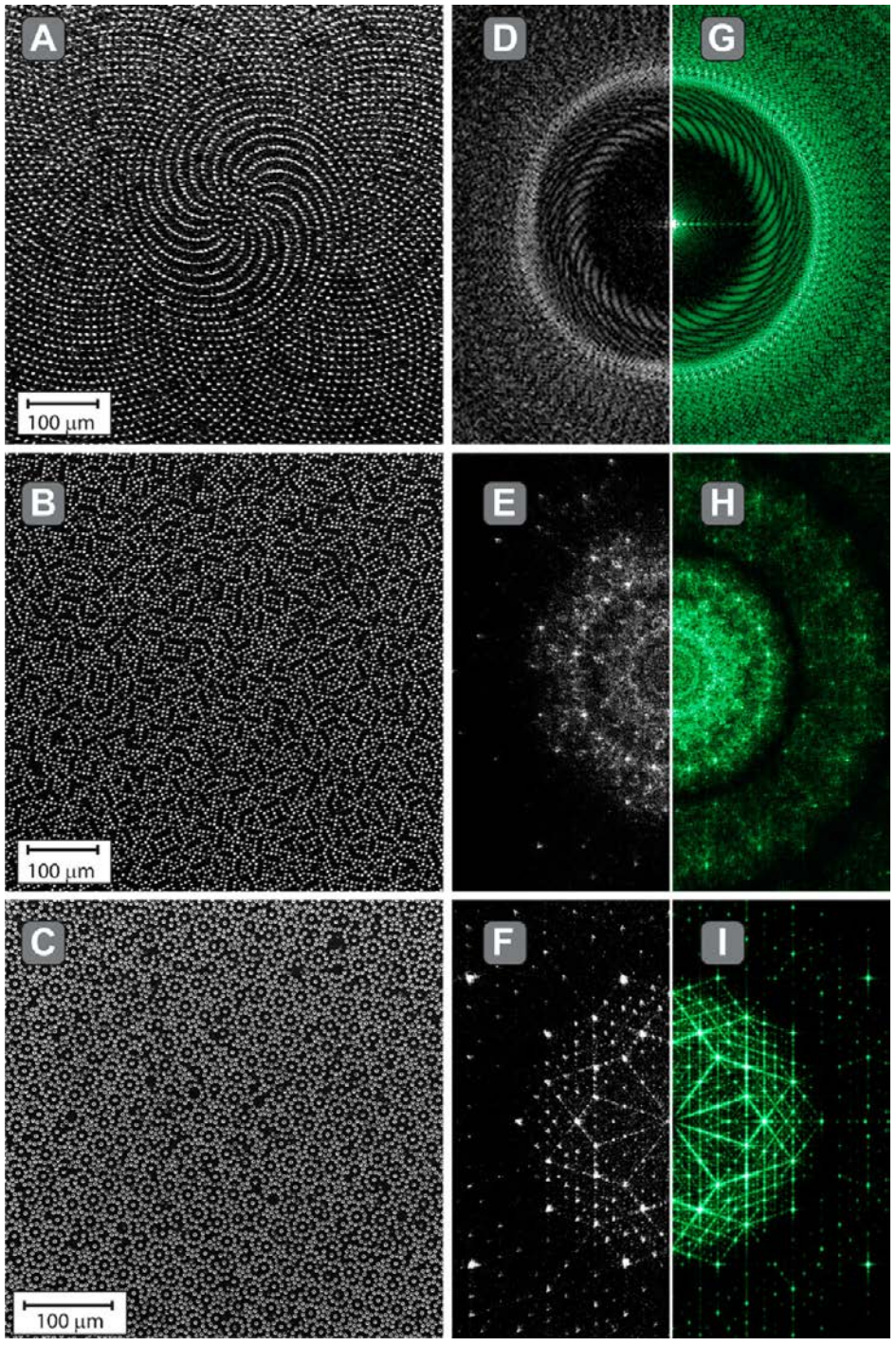

Figure 2. SEM micrograph of three different sample arrays fabricated by TEMPL, showing an α_1-spiral lattice (A), a pinwheel lattice (B), and a Penrose lattice (C). The Fourier transform of the SEM images (D−F), together with those of ideal lattices (G−I), show the overall quality of the nonperiodic lattice structures. Figure 3 shows SEM images of the same samples at a higher magnification.

peeling the PDMS slab from the master. The spheres adhered to the PDMS.

We found that the steps most critical to high quality loading of spheres into wells were (i) the removal of excess PEI from the surface of the wafer and (ii) the proper rubbing of the dry microspheres on the template. Both steps required practice before we were able to reproduce results consistently. To improve the reproducibility of the templated self-assembly of the microspheres further and to minimize the quantity of microspheres required, we believe the steps involving rubbing and transfer could be automated by adapting state-of-the-art transfer printing techniques.[19]

We have noted that the quality of the silicon master templates is critical for the templating process to work efficiently. We obtained our best results with templates in which wells had (i) a diameter as close as possible to 95% of the nominal diameter of the spheres, and (ii) a depth as close as possible to 50% of the diameter of the microspheres. Wider wells could trap the microspheres inside the template and prevent their transfer to the PDMS slabs; narrower wells

DOI: 10.1021/acs.nanolett.6b00952
Nano Lett. 2016, 16, 4125−4132

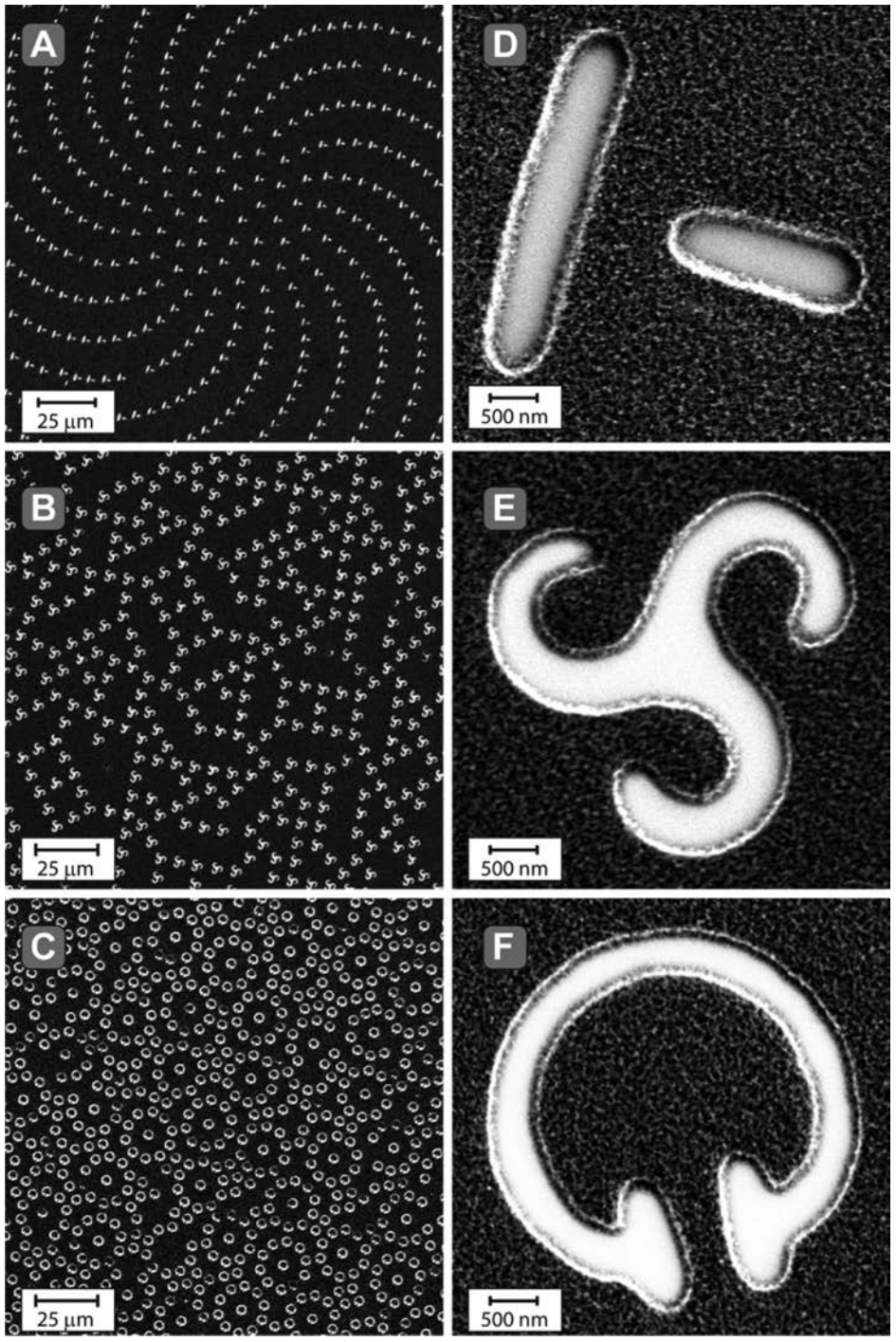

Figure 3. Enlarged SEM micrograph of the three samples from Figure 2 showing an α_1-spiral (A) lattice of T patterns (D), a pinwheel lattice (B) of chiral triskel patterns (E), and a Penrose lattice (C) of split C resonator patterns (F).

reduced the efficiency of loading of the templates; shallower wells prohibited the microspheres from settling in the wells in the template. The SI provides illustration of those problems. We fabricated Si-based templates that were optimized for 5 μm microspheres by using a depth of 2.5 μm and a width of 4.8 μm. Using these templates, the only defects we observed were point defects due to wells that did not have a sphere in a templated position or had one but did not transfer it to the PDMS. The latter problem was more detrimental because the spheres that did not transfer remained permanently stuck inside the corresponding well, and the defects they produced were thus copied to all subsequent substrates that used the same master template for self-assembly.

The rate of defect formation was governed primarily by the experience of the user performing the steps involving the filling of the wells with PEI and the assembly of the microspheres (rubbing) and by the underlying quality of both microspheres and templates (e.g., size of the beads relative to wells). To estimate the quality of template-assisted self-assembly, we performed image analysis of optical micrographs of the templated arrays of microspheres transferred onto PDMS. We analyzed samples selected at random, fabricated by different

DOI: 10.1021/acs.nanolett.6b00952
Nano Lett. 2016, 16, 4125−4132

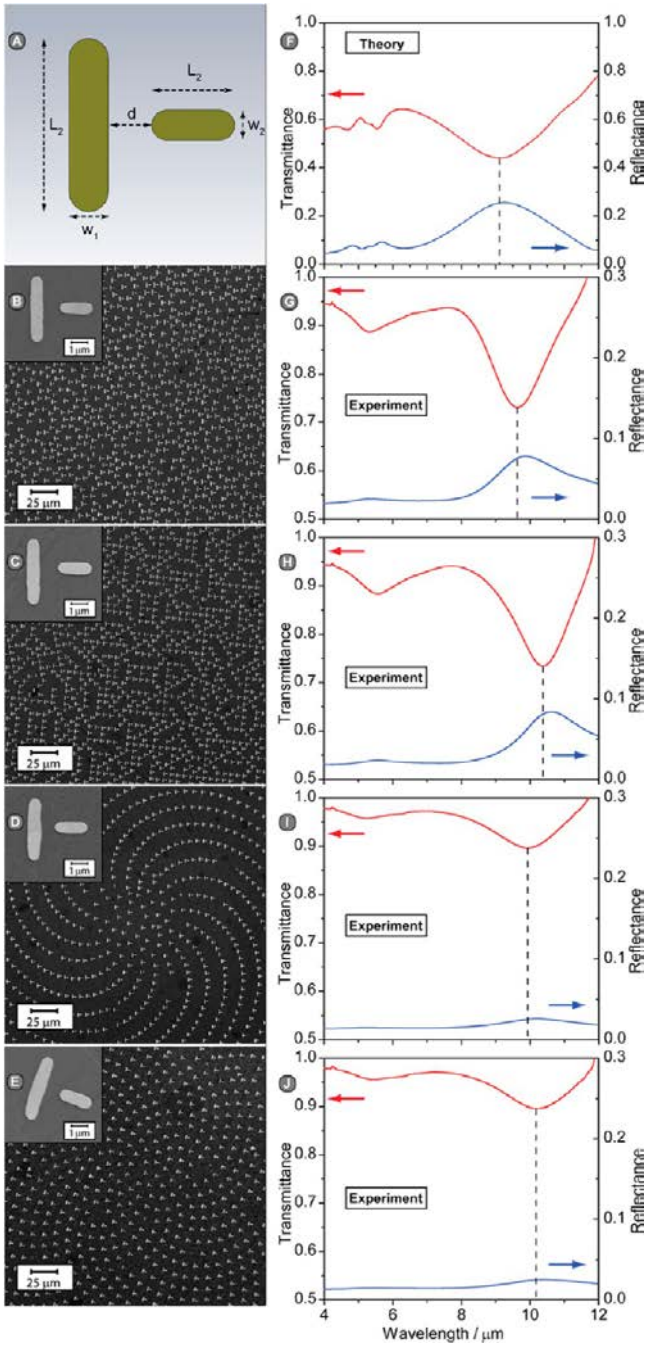

Figure 4. Schematic diagram of a single T-shaped nano pattern (A) and its theoretical transmittance and reflectance IR spectra (F). SEM micrographs (B–E) and optical transmittance and reflectance IR spectra (G–J) for four different arrays of gold T-shaped nanopatterns fabricated on CaF_2.

coauthors at various stages of their experience with the process and throughout the course of the experimental phase of this study. The values we quote here are simply estimates; a detailed analysis of the template-to-template and user-to-user variations is beyond the scope of this study. For an optimized process, we estimate that for inexperienced users (first day trying the process), the average defect rate per sample was <10% (that is, >90% of the spheres were correctly transferred to the PDMS). For more experienced users (several days to weeks of experience), the defect rate was reduced to ~3–5% with no other perceptible distortion to the transferred pattern of spheres (see Figure S2). The most experienced user (the first author) could achieve a further improved defect rate (<3%) for some (~10%) of samples. Regardless of experience, occasionally the defect rate for a single sample was high (>20%), usually due to an overetched template where the wells were too large or too shallow and the microspheres would get trapped or due to a bad batch of microspheres (too large or too high a variability in sphere diameter). In principle, defects caused by size-variation in the microspheres could be reduced further by carefully filtering the microspheres by size (prior to self-assembly) to lower their polydispersity.

In the next phase of TEMPL (steps v–vii in Figure 1a), we used the templated microspheres as microlenses for projection photolithography.[15−17] Figure 1b shows a schematic description of the microlens projection lithography technique that we developed specifically for TEMPL. In more detail, we first prepared photosensitive substrates by spin-coating 200 nm of positive photoresist (from a diluted solution of Shipley S1805 in 1-methoxy-2-propyl acetate, see SI for the detailed experimental parameters) on the silicon substrates. We next coated these substrates with 1500 nm of poly(acrylic acid) (PAA) by spin-coating from an aqueous solution of PAA, see SI. The PAA layer formed a removable spacer[20] that set the focal plane of the microspheres to lie in the photoresist layer. We calculated the thickness of the PAA spacer based on an analytical model that we describe in the Supporting Information. We then brought the arrays of microspheres into direct contact with the PAA layer by carefully placing the PDMS slab (~1 mm thick; spheres side down) on top of the target substrate and did not remove it until after the exposure with UV light.

To perform the patterning, we laser-cut macroscale masks into light-absorbing blackout paper, mounted a mask on a diffuser plate (to ensure homogeneous illumination in all directions) 3 cm above the sample, and exposed it with an intense, uncollimated, UV flood-light (450 mW/cm^2). After exposure, we removed the PDMS slab (including the spheres) manually, removed the PAA layer with water, and developed the patterned photoresist using a conventional photoresist developer. Using this procedure, we fabricated arrays of projected micropatterns with feature sizes down to 400 nm with shapes determined by the macroscale mask and with a spatial arrangement defined by the initial template. The main parameters controlling the process are (i) the thickness of the PAA layer, (ii) the thickness of the photoresist layer, (iii) the distance from the mask to the substrate, (iv) the size and uniformity of the spheres, (v) the exposure time. Some of those parameters are coupled and affect the quality of the projection lithography. In particular, the ideal thickness of the PAA focusing layer depends on the size of the spheres. Altogether, using commercial spheres with a coefficient of variation in size of 5–10%, we found that the quality of the patterns obtained by TEMPL was uniform when using PAA layers with a thickness in the range 1.4–1.6 μm. Finally, the distance between the mask and the substrate controls the magnification and is therefore quite tolerant to small variations. We include further details about methods, optical calculations, and our experimental setup in the Supporting Information.

To demonstrate the applicability of TEMPL, we fabricated four different types of microlens arrays based on well-known, quasiperiodic structures: a Penrose lattice, a pinwheel lattice, and two different Vogel spirals (an α_1 spiral and a golden angle spiral).[4] These patterns provided useful test cases because they

DOI: 10.1021/acs.nanolett.6b00952
Nano Lett. 2016, 16, 4125–4132

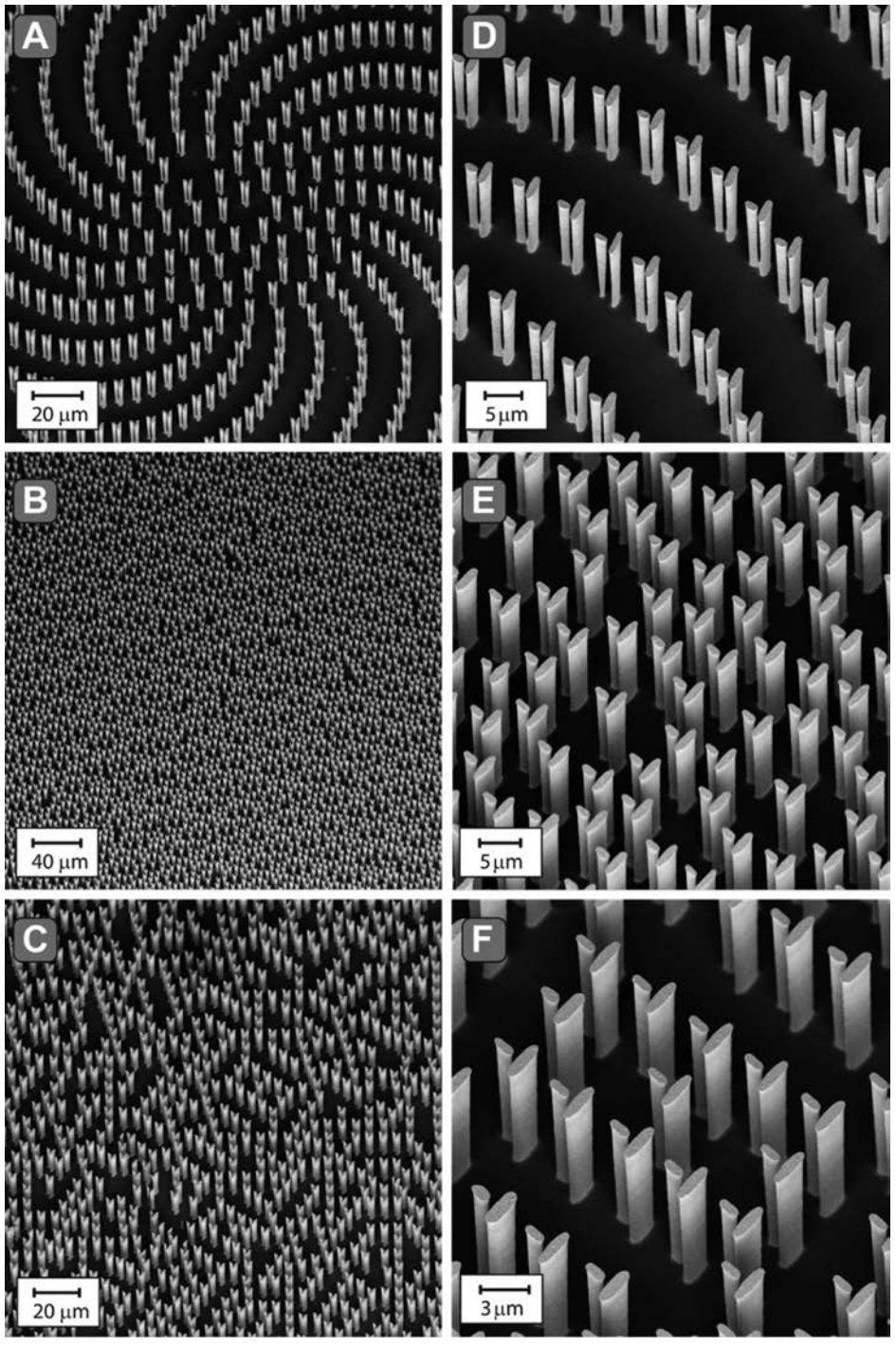

Figure 5. A T-shaped nanopattern that was first patterned in gold on silicon and then etched to yield micropillars using DRIE. The different lattice structures are an α_1 spiral (a,d), a Penrose lattice (b,e), and a pinwheel lattice (c,f).

are complex and known to exhibit interesting optical phenomena.[4,10,21−23] Figure 2 shows scanning electron microscopy (SEM) images of three arrays of nanopatterns etched into photoresist after projection through three different nonperiodic arrays of microspheres.

The sharpness of the Fourier transforms (Figure 2d−f) of the images of the arrays shown in Figure 2a−c confirms the high quality of these patterns.

Figure 3 shows a close-up view of these arrays and demonstrates the quality of the high-resolution nanopatterns obtained locally under each microsphere. Although the exposure time had to be optimized for every mask, this process of optimization was completed relatively quickly each time it was necessary; exposures took only a few seconds and each microlens array, when handled carefully, could be reused multiple times without noticeable degradation in the spatial arrangement of the microspheres. If handled roughly, however, the microlens arrays were damaged and could not be reused.

We next demonstrated the use of TEMPL to produce structures active in the near-infrared. Figure 3d shows the simple T-structure that we chose for the unit cell. We prepared four different nonperiodic metasurfaces with TEMPL and then

DOI: 10.1021/acs.nanolett.6b00952
Nano Lett. 2016, 16, 4125−4132

performed a standard lift-off procedure to metallize the patterns into gold. To simplify infrared optical measurements, we made some minor modifications to the fabrication process. Specifically, we (i) used calcium fluoride disks for the target substrate; (ii) spin-coated a lift-off resin onto the substrates before coating the photoresist; then, after development (iii) used electron beam deposition to lay down an adhesion layer of Ti (5 nm) followed by an active layer of Au (50 nm); and finally, (iv) performed lift-off in warm (~80 °C) *N*-methylpyrrolidone. Figure 4b–e shows the resulting patterns.

We characterized these nonperiodic nanostructure arrays with an FTIR spectrometer and performed simulations by finite integration technique in CST microwave studio (see SI for details about the simulation). Because the global patterns were too complex to simulate, we only simulated spectra for a single unit cell. The measured spectra all showed a primary peak (both transmission and reflection) around 10 μm (Figure 4g–j). Those spectra matched closely with the theoretical spectra (Figure 4f). Slight differences in the position and depth of the peak were likely affected by the global symmetries of the lattices (or lack thereof). The reflectance was weaker than the transmittance, most likely due to loss by the rough top-surface of the nanoantennas. The Penrose and pinwheel lattices provide a stronger signal than the Vogel spirals, most likely because of the higher overall areal density of the Penrose and pinwheel lattices; it is known that packing density has a strong effect on the amplitude of optical spectra in metamaterials.[24]

Finally, to demonstrate the broad applicability of TEMPL further, and in particular the capability of fabricating structures with high aspect-ratios, we performed a deep reactive ion etching step on three metallized samples fabricated on silicon (where the metallic patterns thus served as an etch mask). We used a Bosch etch process[25] that we calibrated to yield a 10 μm deep etch of silicon with vertical sidewalls. Figure 5 shows SEM images of the resulting nonperiodic arrays of metal-capped, vertical structures.

Overall, TEMPL enables rapid and inexpensive fabrication of large area arrays of arbitrarily positioned nanostructures at a low cost and without the need for specialized equipment. When using an unfiltered flood UV-source, the minimum feature size obtained with the microlenses we used was ~0.4 μm. TEMPL enables efficient exploration of the effect of lattice structure on the optical properties of infrared metasurfaces and allows the preparation of both periodic and nonperiodic structures. Moreover, combined with deep reactive ion etching, TEMPL makes it possible to prepare high aspect-ratio features and is therefore suited for the preparation of multilayer stacks as needed, for example, for the fabrication of zero-index metamaterials.[26,27] This method may also enable the rapid fabrication of perfect absorbers for the IR range with important applications to manufacturing efficient IR optics.[28] TEMPL may also be adapted to nonoptical applications, as a convenient alternative method for fabricating nanostructures with feature-sizes ranging between 0.4–5 μm. Possibilities for further development include the use of superlens layers,[29,30] which may open the door to super-resolution imaging with spherical microlenses.[31]

■ ASSOCIATED CONTENT

Supporting Information

The Supporting Information is available free of charge on the ACS Publications website at DOI: 10.1021/acs.nanolett.6b00952.

Background information, experimental details, analytical description of the spherical aberration, and SEM images of additional samples.(PDF)

■ AUTHOR INFORMATION

Corresponding Author

*E-mail: gwhitesides@gmwgroup.harvard.edu.

Notes

The authors declare no competing financial interest.

■ ACKNOWLEDGMENTS

We thank A. A. Stokes, R. Nunes, A. Tayi, and Ozge Akbulut for useful discussions. This work was supported by the Office of Naval Research under award no. N00014-10-1-0942. M.G. acknowledges Marie Curie award SAM-TunEGaIn:IOF-2012-328412. M.H. acknowledges Marie Curie IOF FP7 project nanoPAD (Grant Agreement 330017), the Bo Rydins stiftelse (SCA AB), and the Sweden-America Foundation. L.R. was funded by the REU program under National Science Foundation (NSF) award No. DMR-1420570. This work was performed in part at the Center for Nanoscale Systems (CNS), a member of the National Nanotechnology Infrastructure Network (NNIN), which was supported by NSF award no. ECS-0335765. CNS is part of Harvard University.

■ REFERENCES

(1) Kildishev, A. V.; Boltasseva, A.; Shalaev, V. M. *Science* **2013**, *339*, 1232009.

(2) Holloway, C. L.; Kuester, E. F.; Gordon, J. A.; O'Hara, J.; Booth, J.; Smith, D. R. *IEEE Antennas Propag. Mag.* **2012**, *54*, 10–35.

(3) Jahani, S.; Jacob, Z. *Nat. Nanotechnol.* **2016**, *11*, 23–36.

(4) Dal Negro, L.; Boriskina, S. V. *Laser Photonics Rev.* **2012**, *6*, 178–218.

(5) Lipworth, G.; Ensworth, J.; Seetharam, K.; Da, H.; Lee, J. S.; Schmalenberg, P.; Nomura, T.; Reynolds, M. S.; Smith, D. R.; Urzhumov, Y. *Sci. Rep.* **2014**, *4*, 3642.

(6) Yanik, A. A.; Cetin, A. E.; Huang, M.; Artar, A.; Mousavi, S. H.; Khanikaev, A.; Connor, J. H.; Shvets, G.; Altug, H. *Proc. Natl. Acad. Sci. U. S. A.* **2011**, *108*, 11784–11789.

(7) Xu, X.; Peng, B.; Li, D.; Zhang, J.; Wong, L. M.; Zhang, Q.; Wang, S.; Xiong, Q. *Nano Lett.* **2011**, *11*, 3232–3238.

(8) Wu, C.; Khanikaev, A. B.; Adato, R.; Arju, N.; Yanik, A. A.; Altug, H.; Shvets, G. *Nat. Mater.* **2011**, *11*, 69–75.

(9) Kravets, V. G.; Schedin, F.; Jalil, R.; Britnell, L.; Gorbachev, R. V.; Ansell, D.; Thackray, B.; Novoselov, K. S.; Geim, A. K.; Kabashin, A. V.; et al. *Nat. Mater.* **2013**, *12*, 304–309.

(10) Dal Negro, L. *SPIE Newsroom* **2012**, DOI: 10.1117/2.1201206.004306.

(11) Xie, L.; Gao, W.; Shu, J.; Ying, Y.; Kono, J. *Sci. Rep.* **2015**, *5*, 8671.

(12) Aieta, F.; Genevet, P.; Kats, M. A.; Yu, N.; Blanchard, R.; Gaburro, Z.; Capasso, F. *Nano Lett.* **2012**, *12*, 4932–4936.

(13) Yu, N.; Capasso, F. *Nat. Mater.* **2014**, *13*, 139–150.

(14) Lin, D.; Fan, P.; Hasman, E.; Brongersma, M. L. *Science* **2014**, *345*, 298–302.

(15) Wu, M.-H.; Whitesides, G. M. *Appl. Phys. Lett.* **2001**, *78*, 2273–2275.

(16) Wu, M.-H.; Whitesides, G. M. *J. Micromech. Microeng.* **2002**, *12*, 747–758.

(17) Wu, M.-H.; Park, C.; Whitesides, G. M. *J. Colloid Interface Sci.* **2003**, *265*, 304–309.

(18) Khanh, N. N.; Yoon, K. B. *J. Am. Chem. Soc.* **2009**, *131*, 14228–14230.

(19) Carlson, A.; Bowen, A. M.; Huang, Y.; Nuzzo, R. G.; Rogers, J. A. *Adv. Mater.* **2012**, *24*, 5284–5318.

DOI: 10.1021/acs.nanolett.6b00952
Nano Lett. 2016, 16, 4125–4132

(20) Linder, V.; Gates, B. D.; Ryan, D.; Parviz, B. A.; Whitesides, G. M. *Small* **2005**, *1*, 730−736.
(21) Dal Negro, L. *Optics of aperiodic structures: fundamentals and device applications*; Pan Stanford: Singapore, 2014.
(22) Dal Negro, L.; Lawrence, N.; Trevino, J. Engineering Aperiodic Spiral Order in Nanophotonics: Fundamentals and Device Applications. In *Nanodevices for Photonics and Electronics*; Bettotti, P., Ed.; Pan Stanford: Singapore, 2015; pp 57−125.
(23) Dal Negro, L.; Lawrence, N.; Trevino, J. Engineering the Orbital Angular Momentum of Light with Plasmonic Vogel Spiral Arrays. In *Singular and Chiral Nanoplasmonics*; Boriskina, S., Zheludev, N. I., Eds.; Pan Stanford: Singapore, 2014; pp 335−374.
(24) Singh, R.; Rockstuhl, C.; Zhang, W. *Appl. Phys. Lett.* **2010**, *97*, 241108.
(25) Laermer, F.; Schilp, A. Method of anisotropically etching silicon. U.S. Patent 5,501,893, 1996.
(26) Li, Y.; Kita, S.; Muñoz, P.; Reshef, O.; Vulis, D. I.; Yin, M.; Lončar, M.; Mazur, E. *Nat. Photonics* **2015**, *9*, 738−742.
(27) Moitra, P.; Yang, Y.; Anderson, Z.; Kravchenko, I. I.; Briggs, D. P.; Valentine, J. *Nat. Photonics* **2013**, *7*, 791−795.
(28) Liu, N.; Mesch, M.; Weiss, T.; Hentschel, M.; Giessen, H. *Nano Lett.* **2010**, *10*, 2342−2348.
(29) Fang, N.; Lee, H.; Sun, C.; Zhang, X. *Science* **2005**, *308*, 534−537.
(30) Zhang, X.; Liu, Z. *Nat. Mater.* **2008**, *7*, 435−441.
(31) Li, S.; Du, C.; Dong, X.; Shi, L.; Luo, X.; Wei, X.; Zhang, Y. *Opt. Express* **2008**, *16*, 14397−14403.

DOI: 10.1021/acs.nanolett.6b00952
Nano Lett. 2016, 16, 4125−4132